X-RAY STRUCTURE STUDY OF THERMOTROPIC PHASES IN ISOACYLPHOSPHATIDYLCHOLINE MULTIBILAYERS

S. E. CHURCH,* D. J. GRIFFITHS,* R. N. A. H. LEWIS,‡ R. N. MCELHANEY,‡ AND H. H. WICKMAN*

*Departments of Chemistry, Physics, and Biochemistry, Oregon State University, Corvallis, Oregon 97331; and ‡Department of Biochemistry, University of Alberta, Edmonton, Alberta, Canada T6G 2H7

ABSTRACT Structures of lamellar phases in aqueous dispersions of diisoacylphosphatidylcholines (17iPC and 20iPC) were determined by x-ray diffraction methods. In agreement with previous DSC studies, subgel, gel, and liquid crystal phases were observed in each homolog. The subgel Lc(c') phases of both homologs show significant two-dimensional long range order and can be described by rectangular lattices. The dimensions of the two rectangular unit cells differ in that the side chains are canted (~33°) in the 20iPC homolog, while in 17iPC the side chains are normal to the bilayer plane. The gel Lβ phases of 17iPC (T_{gg} = 17–19.5°C) and 20iPC (T_{gg} = 44°C) are similar but not identical and are consistent with a distorted, pseudohexagonal lattice for the rotationally disordered side chains. The liquid crystal phases of 17iPC (T_{gl} = 28°C) and 20iPC (T_{gl} = 52°C) are structurally similar and are typical of lipids with fluid side chains. Significant but different changes occur in the long spacings at T_{gg} and T_{gl} for the two homologs. This implies that interfacial states (particularly in the subgel phases) differ in the two homologs below the liquid crystal phase transition temperature.

INTRODUCTION

The phase behavior of lipid bilayers formed by phosphatidylcholines containing methyl iso- and anteisobranched fatty acyl chains is of interest from both structural and biochemical viewpoints. Aspects of thermotropic phase behavior in these materials have been established by a number of physical techniques (1–4). The most completely studied system is the series of diisoacylPCs (niPCs, with n = 15–22) (2, 3). This work showed that the thermal properties of iso-branched PCs differ from those of common straight chain PCs (nPCs), such as dipalmitoylphosphatidylcholine (DPPC). Possible structural details of these differences were inferred from Infrared (IR) and ^{31}P-Nuclear Magnetic Resonance (NMR) spectroscopic techniques (3). Biochemical interest in branched fatty acids arises from their widespread occurrence in certain bacteria, particularly eubacteria (5). Further, it has been suggested that methyl iso- and anteisobranched fatty acyl groups may influence the properties of lipids of certain bacterial membranes in ways analogous to linear saturated and monounsaturated acyl side chains (5).

The iso-branched PCs show two thermal phase transitions, the lower of which (T_{gg}) is ascribed to a transition between two gel phases, and the higher of which (T_{gl}) corresponds to the expected gel to liquid crystal phase transition observed in most lipids. We refer to the three phases as subgel, gel, and liquid crystal. T_{gl} is decreased significantly with respect to nPCs of similar carbon number. The temperature separation between the two transitions in iPCs varies in a nonlinear manner with the number of carbon atoms in the side chains, and in some cases (15iPC, 16iPC, and 18iPC) T_{gg} and T_{gl} are nearly coincident (2). However, T_{gg} and T_{gl} are well separated in the 17iPC and 20iPC homologs, the subjects of this study. The thermodynamic characterization (2) of the two phase transitions suggests that the gel to liquid crystal phase transition is similar to that observed in nPCs. However, there are pronounced differences between the subgel to gel phase transition and possible corresponding phase transitions in DPPC, such as the pretransition (6, 7) or subtransition (8–13). IR spectroscopic data (3) have been interpreted as showing profound conformational differences between gel states of odd (number of carbon atoms in side chain) and even chain species.

Although characterized thermodynamically, and by IR and NMR spectroscopic techniques, a direct structural investigation of the long range order in iso-branched PCs has been lacking. We report here an x-ray structure

[1] *Abbreviations used in this paper*: DPPC: 1,2-dipalmitoyl-*sn*-glycero-3-phosphorylcholine; DSC: Differential scanning calorimety; IR: Infrared; MLV: Multilamellar vesicle; NMR: Nuclear magnetic resonance; *n*iPC, n = 15–22: 1,2-diisoacyl-*sn*-glycero-3-phosphorylcholine, where n denotes the number of carbon atoms in the isoacyl side chain; *n*PC, n = 14–21: 1,2-diacyl-*sn*-glycero-3-phosphorylcholine, where n denotes the number of carbon atoms in the acyl side chain; PC: 1,2-diacyl-*sn*-glycero-3-phosphorylcholine; PSD: Position sensitive detector; S: Effective side chain area; S_o: Limiting, close-packed side chain area; T_{gg}: Subgel to gel phase transition temperature; T_{gl}: Gel to liquid crystal phase transition temperature; θ: Angle of the side chain axes with respect to the bilayer normal.

investigation of dispersions of the 17iPC and the 20iPC homologs in excess water. The data allow a classification of the lamellar structure of the subgel, gel, and liquid crystal phases in terms of nomenclature developed to describe phases in nPCs (11, 14, 15). The results provide a clear picture of structure differences between lamellar phases of even and odd chain iPCs and between corresponding phases in nPCs.

METHODS AND MATERIALS

Sample Preparation

The lipids were synthesized as previously described (2). The dry lipid was dissolved in benzene and the solution evaporated with nitrogen gas to yield a clear film in a glass flask. The lipid was then dried by overnight vacuum desiccation. The resulting deposit was hydrated with excess distilled and millipore-filtered water, heated above T_{gl}, and maintained at that temperature for 20 to 60 min, with intermittent vortexing (1 min, total time). The suspension was cooled to room temperature and centrifuged at 1,500 g for 20 min to obtain a pellet of multilamellar vesicles (MLVs). The MLVs were transferred to x-ray capillary tubes (1 mm diameter with 0.01 mm wall), centrifuged at low speeds and most of the excess supernatant water removed. Finally, the capillary tubes were flame sealed and centrifuged at 5,500 g to concentrate the lipid dispersion for x-ray study. Samples were stored at 4°C for at least 24 h prior to x-ray experiments. In all cases, the specimen was annealed at 0°C in the variable temperature diffraction stage until both wide angle and low angle x-ray patterns were stable.

X-ray Methods

Pin-hole collimation and nickel filtered CuKα radiation were used. The x-rays were detected with two position sensitive flow proportional counters (PSDs) of local design and construction (16). The detectors have an active length of 100 mm and an efficiency of >90% for 8 KeV radiation. One detector was placed ~200 mm from the sample and intercepted the low angle region (1/150 Å^{-1} to 1/6 Å^{-1}). The second detector was placed ~280 mm from the sample at an angle of 20° to the beam and intercepted diffraction lines in the wide angle region (1/3 Å^{-1} to 1/7 Å^{-1}). Programs were written to correct the low angle data from minor nonlinearities in the PSDs and for small distortions arising from variations in acceptance angles among different orders of diffraction. The wide angle detector geometry was calibrated with a calcite diffraction pattern. The variable temperature sample stage had an accuracy of ±0.2°C and a stability of ±0.1°C.

EXPERIMENTAL RESULTS

17iPC

Upon initial cooling from ambient to 0°C, all samples showed some thermal annealing effects. The lamellar repeat distance quickly (~6–10 h) decreased to a constant value, while the wide angle pattern showed slow (12–16 h) changes in the relative intensities of the various reflections. These time dependent effects, which reflect molecular ordering dynamics in the two-dimensional lattice described below, are under continuing study. After 16 h, the spectrum was stable. Within experimental statistics, all samples showed the same wide angle reflections, but from sample to sample there was some variation in the relative intensities in both the region near 1/4.5 Å^{-1}, which is characteristic of the interchain reflection, and the remainder of the wide angle region, which reflects two dimensional order of the intrabilayer molecular packing.

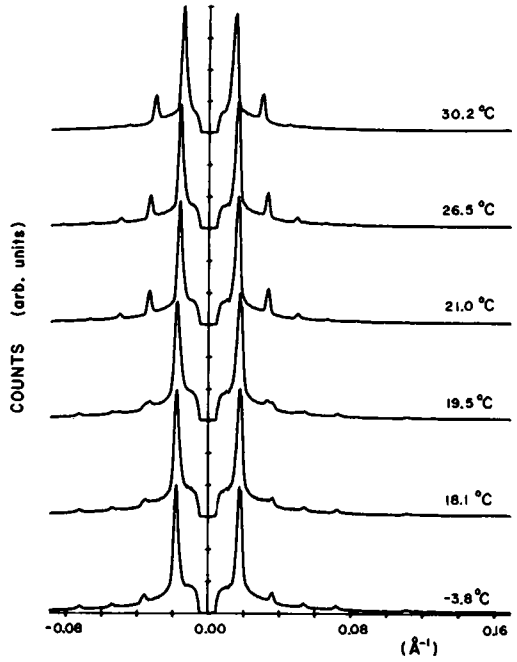

FIGURE 1 Low angle x-ray patterns for MLVs of 17iPC in excess water. Sample temperatures are indicated.

Low angle diffraction patterns for several sample temperatures are given in Fig. 1. Wide angle patterns are given in Fig. 2. The x-ray data show clear evidence of phase transitions at 19.5°C and 28.0°C. FT-IR studies also show transitions at these temperatures (3). On the other hand,

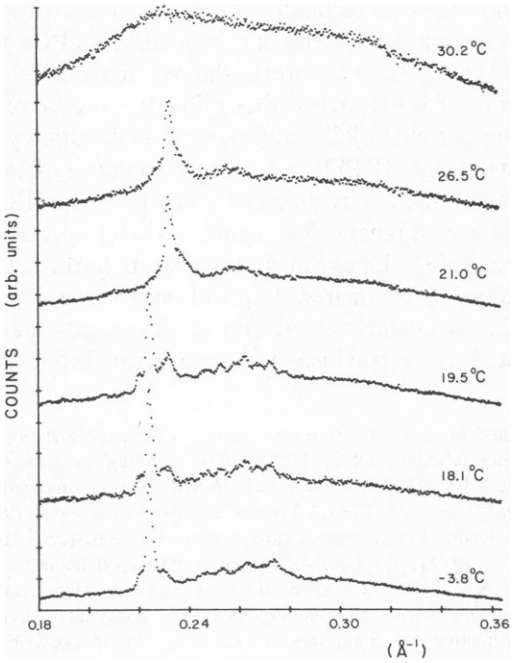

FIGURE 2 Wide angle x-ray patterns for MLVs of 17iPC in excess water. Sample temperatures are indicated.

the original DSC investigation identified a subgel to gel transition near 15°C and a gel to liquid crystal transition at 28.0°C (2). Because of the discrepancy between measured values of the subgel-gel transition, the DSC properties of the 17iPC have been reinvestigated. It has been found that the DSC scans are sensitive to annealing procedures. In the earlier work, the samples were annealed (prior to DSC scans) for at least 24 h at a temperature of 3 to 4°C. In the present x-ray work, samples have been annealed in the sample chamber for at least 24 h (at 0°C), until the diffraction patterns were stable. With a similar, low temperature anneal prior to DSC scan, the result shown in Fig. 3 is obtained. The DSC scan shows a broad transition, centered at 20.5°C with $\Delta H \simeq 6$ kcal/mol. The scan rate was 0.31°C/min. This T_{gl} compares favorably with the subgel-gel transition observed in the x-ray and FT-IR work. The breadth of the transition is consistent with the x-ray work, which shows a coexistence of subgel and gel phases at T_{gl} (Fig. 1). Additional x-ray measurements are in progress, using variable annealing cycles, to characterize structurally the subgel-gel transition at 16°C.

It is evident from the low angle data that a high degree of lamellar order is present. The wide angle data also show significant structure, indicating that the isoacyl side chains are well ordered at temperatures below T_{gl}. Evidence of order is most pronounced in the subgel phase.

We consider first the diffraction data from the subgel phase. In addition to the lamellar diffraction, the low angle data show a characteristic peak near 1/9.10 $Å^{-1}$ with a much weaker shoulder at 1/8.75 $Å^{-1}$ and weak line at 1/6.31 $Å^{-1}$. These peaks do not index as higher order reflections from the lamellar structure. They disappear upon heating the sample through T_{gg} and are taken as a signature of the subgel phase in 17iPC. The wide angle data show several lines. Because exposure times varied, not all peaks are resolved in every pattern. In the subgel phase, at least five reflections can be distinguished: 1/4.55, 1/4.40, 1/4.05, 1/3.90, and 1/3.78 $Å^{-1}$. It is significant that the sharpest line occurs at 1/4.55 $Å^{-1}$. As discussed below, this reflection gives information about the mode of side chain packing.

The subgel to gel transition leads to a new wide angle pattern, less well resolved and characterized by a new, sharp line at 1/4.40 $Å^{-1}$ and a broad line at 1/3.85 $Å^{-1}$. Upon increasing the temperature to 28.0°C, the gel to liquid crystal phase transition occurs and the pattern

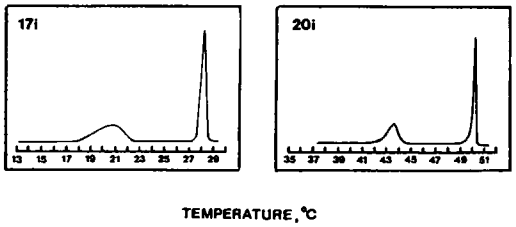

FIGURE 3 DSC profiles for 17iPC and 20iPC.

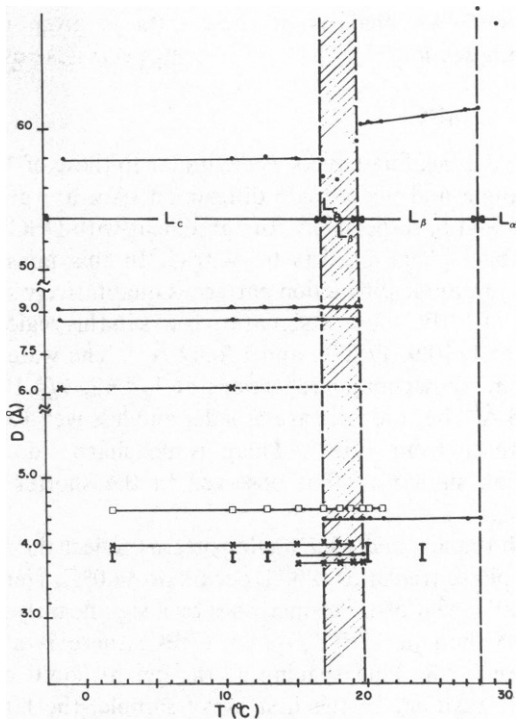

FIGURE 4 Temperature variation of the observed diffraction lines of MLVs of 17iPC in excess water.

reduces to a broad weak line at 1/4.5 $Å^{-1}$ characteristic of the fluid state for the hydrocarbon side chains.

The temperature variation of the various reflections is given in Fig. 4. The lamellar repeat distance increases slightly at T_{gg} and strikingly at T_{gl}. Table I lists major

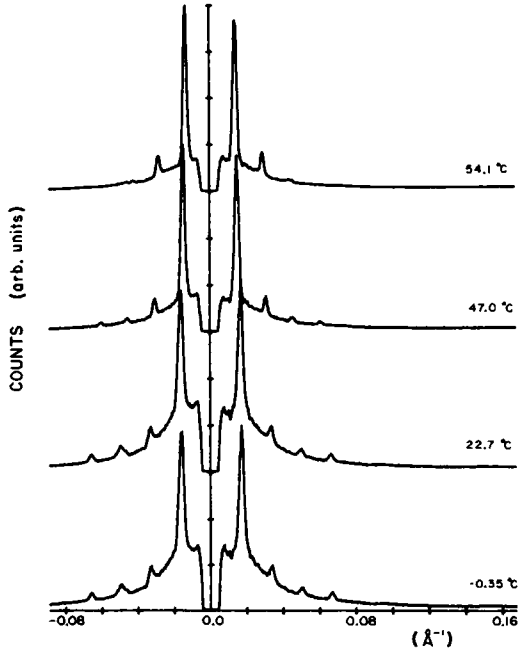

FIGURE 5 Low angle x-ray patterns for MLVs of 20iPC in excess water. Sample temperatures are indicated.

reflections. An analysis of these data is given in the following section.

20iPC

Thermal annealing effects were similar to those of 17iPC. Low angle and wide angle diffraction data are given in Figs. 5 and 6, respectively. In agreement with DSC work, the subgel phase persists to 44.0°C. In this phase, the 20iPC low angle diffraction pattern is qualitatively similar to that of 17iPC, but the signature peaks in this region now occur at 1/10.9, 1/8.75, and 1/6.82 $Å^{-1}$. The wide angle spectrum shows major reflections at 1/4.62, 1/4.12, and 1/3.75 $Å^{-1}$ but the lines are broader and less well-resolved than those from 17iPC. There is no sharp side chain reflection similar to that observed in the shorter chain homolog.

Both the low and wide angle patterns reflect the subgel to gel phase transition which occurs at 44.0°C. Here, the lamellar repeat distance increases by a significantly larger amount than in 17iPC. As in 17iPC, there is a large increase in the long spacing at the gel to liquid crystal phase transition. In the first x-ray sample, the lamellar order decreased or was lost completely at temperatures above T_{gl} (52.0°C). This may have been due to hydrolysis or other chemical events to which the iPCs are sensitive at higher temperatures (2). In subsequent work, only one point was recorded at a temperature above T_{gl}.

DISCUSSION

Because of the absence of three dimensional long range order in the MLVs, the diffraction data represent different aspects of the partial order of the lipid/water organization. The low angle region reflects the degree of lamellar order while the wide angle region near 1/4.5 $Å^{-1}$ provides information about the side chain conformation (cant angle and fluid state) (6). These data are used below to assign the lamellar structure in terms of conventional notation (11, 14, 15). In the subgel phases, where there is significant intrabilayer two-dimensional order, it is possible to index wide and low angle lines according to a rectangular lattice. This information is used to determine the side chain cant angle in these phases. Where possible, we comment on thermodynamic and spectroscopic data (2, 3) related to the structural features identified here. In general, there is excellent agreement between that information and the present results.

Subgel Phases

The lamellar repeat distances of 17iPC and 20iPC given in Figs. 4 and 7 are typical of phosphatidylcholine multibilayer dispersions in excess water (14). The repeat distance of 58.0 Å in 17iPC compares with the value 59.5 Å observed in subgel (excess water) DPPC (9–12). The latter phase is denoted Lc, to indicate a lamellar structure, together with a high degree of intrabilayer two-dimensional order (10). This order is presumed to be associated with the side chain arrangement (10, 12). Table I gives the unit cell parameters and indexed reflections in 17iPC, 20iPC, and DPPC.

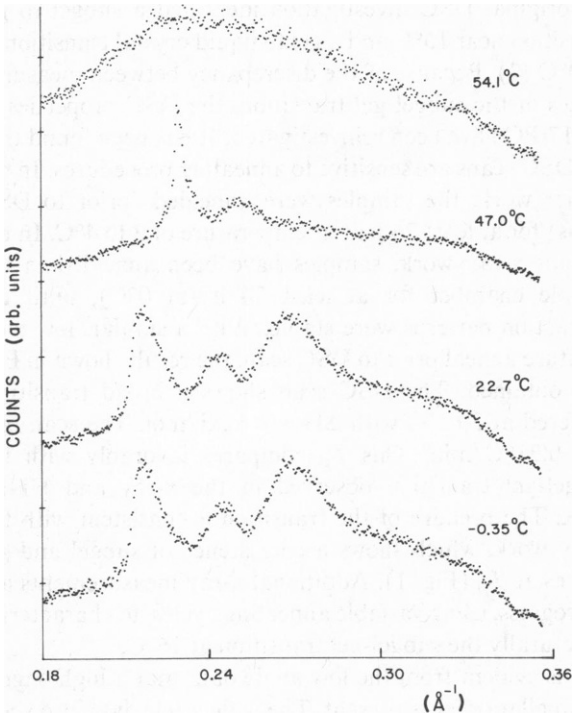

FIGURE 6 Wide angle x-ray patterns for MLVs of 20iPC in excess water. Sample temperatures are indicated.

Information about side chain state is derived from analysis of the reflections in the two-dimensional lattice that can be associated with interchain distances and by an analysis of the two-dimensional lattice (given below). A sharp wide angle line (in fact the sharpest line) at 1/4.55 $Å^{-1}$ is found in 17iPC but not in 20 iPC. This line corresponds to a spacing of one-half of the larger unit cell dimension given in Table I. A sharp line can indicate a reflection due to rods or chains with axes normal or near normal to the bilayer plane (6). However, if the side chains are canted with respect to the bilayer normal, the interchain reflection becomes broadened and somewhat shifted (6, 17). There is no corresponding sharp line in 20iPC but in its place is a broad line at 1/4.63 $Å^{-1}$. On this basis, it is possible to conclude that the side chains in 20iPC are canted, while in 17iPC they are near normal to the bilayer plane. This result is also consistent with an analysis of the two-dimensional order given below.

The picture of subgel 17iPC and 20iPC that emerges from the x-ray data is summarized in Fig. 8. In both cases there is a high degree of two-dimensional order, although the side chains are canted in the 20iPC, but not in the 17iPC. The phases are therefore donated Lc′ and Lc, respectively. For reasons noted earlier, we have not yet performed hydration studies of the iPCs, nor are partial specific volumes available. However, the hydration state of

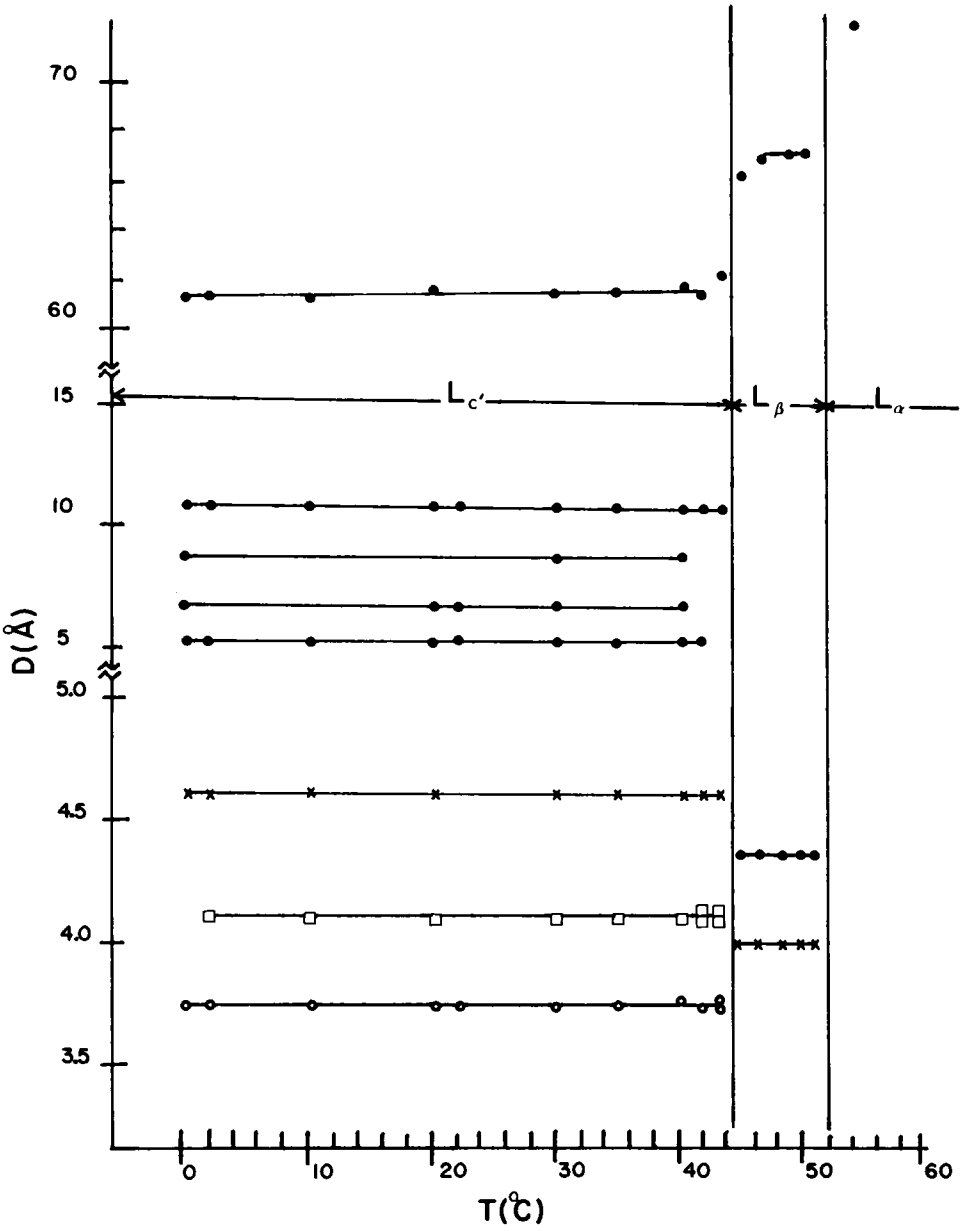

FIGURE 7 Temperature variation of the observed diffraction lines of MLVs of 20iPC in excess water.

the subgel phases can be estimated and the relative hydration states of 17iPC and 20iPC can be determined unambiguously. Using group volumes (6, 18, 21) and molecular models, we estimate the volume of 17iPC as 1,125 $Å^3$ and the volume of 20iPC as 1,250 $Å^{-3}$. A three-dimensional unit cell volume can be obtained from the bilayer repeat distances and the two-dimensional unit cell parameters given in Table I. With a rough estimate of a water molecule volume of 30 $Å^3$, we find in this fashion 0–2 molecules of H_2O associated with 17iPC and 7–8 molecules associated with 20iPC.

It is desirable to compare the iPC hydration levels with that of DPPC. Results of x-ray experiments using DPPC samples in excess water are also summarized in Table I and Fig. 8. The rectangular unit cell parameters quoted in Table I are in agreement with results reported by Fuldner (9), Stümpel et al. (12), and Ruocco and Shipley (10). The wide angle patterns for the DPPC samples annealed at 0°C in excess water are consistent only with canted acyl side chains. Using the three-dimensional unit-cell volume and arguments given above for 17iPC and 20iPC we find ~10 molecules of H_2O associated with each subgel DPPC molecule in excess water. This estimate agrees with the data of Ruocco and Shipley, who by direct hydration studies, found a limiting state for the Lc phase of DPPC corresponding to 11 water molecules (11). It is clear that 17iPC is substantially less, and 20iPC somewhat less, hydrated than DPPC.

The x-ray results for the iPCs are consistent with IR work which showed that the side chains in 17iPC and

TABLE I
OBSERVED X-RAY REFLECTIONS

	Å
A. 17iPC	
Subgel Lc phase	
Lamellar repeat distance:	d = 58.0
Two-dimensional structure:	
Rectangular unit cell:	a = 9.10, b = 8.75
Observed reflections:	9.10, 8.75, 6.31, 4.55, 4.40, 4.05, 3.22
Calculated:	9.10, 8.75, 6.31, 4.55, 4.38, 4.04, 3.94
Index	(1,0) (0,1) (1,1) (2,0) (0,2) (2,1) (1,2)
Interchain relection:	4.55 (very sharp)
Gel Lβ Phase	
Lamellar repeat distance:	d = 61.0
Interchain reflection:	4.40 (sharp), 3.85 (broad)
Liquid Crystal Lα Phase	
Lamellar repeat distance:	d = 67.0
Interchain reflection:	4.5 (very broad)
B. 20iPC	
Subgel Lc′ phase	
Lamellar repeat distance:	d = 61.8
Two-dimensional structure:	
Rectangular unit cell:	a = 10.9, b = 8.75
Observed reflections:	10.9, 8.75, 6.82, 5.30, 4.62, —, 4.12, 3.75
Calculated:	10.9, 8.75, 6.82, 5.45, 4.63, 4.39, 4.06, 3,63
Index	(1,0) (0,1) (1,1) (2,0) (2,1) (0,2) (1,2) (3,0)
Interchain reflection:	4.63 (broad)
Gel Lβ phase	
Lamellar repeat distance:	d = 67.2
Interchain reflections:	4.40 (sharp), 4.00 (broad)
Liquid Crystal Lα Phase	
Lamellar repeat distance:	d = 72.3
Interchain reflection:	4.5 (very broad)
C. DPPC	
Subgel Lc′ phase	
Lamellar repeat distance:	d = 59.5
Two-dimensional structure:	
Rectangular unit cell:	a = 10.1, b = 9.06
Interchain reflections:	4.41 (broad), 3.85 (broad)
Gel Lβ' phase	
Lamellar repeat distance:	d = 63.5
Interchain reflection:	4.20 (sharp)
Gel Pβ' phase	
Lamellar repeat distance:	d = 72.3
Interchain reflection:	4.20 (broad)
Liquid Crystal Lα Phase	
Lamellar repeat distance:	d = 66.5
Interchain reflection:	4.5 (very broad)

20iPC were highly ordered in a manner typical of partially dehydrated phospholipids (3). The IR work further showed that the side chain packings were different in the two homologs. However, it was not possible to establish a specific packing structure on the basis of this data. The carbonyl stretch frequency studies showed that a band at 1,716 cm^{-1} was present in subgel 20iPC but absent in subgel 17iPC. From this it was inferred that there were considerable differences in the subgel state interfacial head group structure between even and odd carbon homologs. The 1,716 cm^{-1} band has been observed in the IR spectra of phospholipids of low hydration state (19). In the present case, however, it is absent in the iPC homolog of lowest hydration level. It is also absent in subgel DPPC (20). Its absence in these cases must therefore be related to the head group conformation. In any case, it seems clear from all the evidence that the head group state (degree of hydration and conformation) is different in 17iPC and 20iPC, and that these states may differ from others observed at lower or higher hydration levels.

Two-dimensional Order

In the Lc (Lc′) phases, the nonlamellar and nonside chain reflections observed in the low angle and wide angle regions can be related to a two-dimensional lattice as shown in Table I. With the reasonable assumption that the two-dimensional order reflects head group and side chain

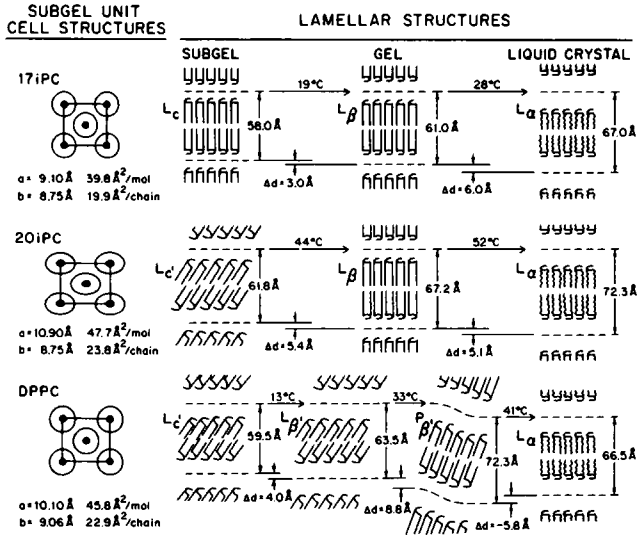

FIGURE 8 Proposed rectangular unit cell structures in the subgel phases and schematic representations of the lamellar structures in the subgel, gel, and liquid crystal phases for MLVs of 17iPC, 20iPC, and DPPC in excess water.

organization within the bilayer plane, the unit cell data can be used to obtain the molecular area. With $a = 9.10$ Å and $b = 8.75$ Å and two molecules per unit cell, the molecular area for 17iPC is 39.8 Å^2 and the effective side chain area S is 19.9 Å^2. Under similar hydration conditions for MLVs of 20iPC and DPPC, the corresponding side chain areas are 23.8 and 22.9 Å^2, respectively. Since the minimum cross sectional area S_0 for an all-*trans* configuration side chain is ~20 Å^2, it is clear that side chain canting occurs in 20iPC and DPPC, while the chains in 17iPC are nearly normal to the bilayer plane. Simple geometrical considerations lead to the relation between side chain cant angle θ, S, and S_0: $S_0/S = \cos\theta$. Thus for 20iPC and DPPC, we estimate the side chain cant angles as 33° and 29°, respectively. The cant angle for 20iPC is markedly lower than the value observed in crystals of isoacyl fatty acids. For example, the angle in 17-methyloctadecanoic acid is 46° (21). The large difference is not surprising since the acyl side chains in the iPCs are certainly influenced by their bonding to the head group in these molecules.

The side chain canting in 20iPC can be related to the rectangular unit cell sizes of 17iPC and 20iPC. It is seen from Table I that the b dimensions are identical in the two cells, while the a dimension of 20iPC is increased over that of 17iPC. This can be accounted for by assuming that the two cells are related and that a rotation of the side chains about the crystallographic b axis distinguishes the 20iPC cell from the 17iPC cell.

Because the cells are related, the cant angle information can be used to obtain additional information about hydration levels in 17iPC and 20iPC. In the 17iPC subgel phase, a simple elongation of the chain by three CH_2 groups of 1.25-Å length followed by rotation of the side chains to the 20iPC cant angle leaves the repeat distance d essentially unchanged. The observed difference between 20iPC and 17iPC subgel d spacing is 3.8 Å. This is consistent with the higher hydration level calculated above for 20iPC.

Gel Phases

Upon heating either 17iPC or 20iPC through T_{gg}, a subgel to gel phase transition occurs. In 17iPC an increase in lamellar repeat distance of 3.0 Å occurs. In 20iPC the increase is larger, 5.4 Å. This behavior distinguishes the two materials and reflects chain reorientation and interfacial events as discussed below. First, it is necessary to establish the side chain state in the two homologs.

The gel phase diffraction properties of both homologs are similar and are typical of a distorted hexagonal side chain lattice. The detailed structure of the Lc phase reflecting long range two-dimensional order has disappeared. The wide angle patterns now exhibit a sharp reflection at 1/4.40 Å^{-1} and broad bands at 1/3.85 Å^{-1} (17iPC) or 1/4.00 Å^{-1} (20iPC). This shows that the gel states of the side chains in the two homologs are rather similar. By analogy with many previous discussions of nPCs, wide angle data of this type may be interpreted in terms of a distorted hexagonal lattice of all-*trans* acyl side chains with chain axes normal to the bilayer plane. There is rotational disorder from chain to chain. These structures are denoted Lβ. It is interesting that the two prominent wide angle lines of gel phases of 17iPC and 20iPC occur at positions almost identical to the two prominent wide angle lines in subgel phase DPPC (9–12; Table I). Indeed, the gel phase of the iPCs can be interpreted as corresponding to a subgel phase DPPC in which the long range order has been lost because of rotational disorder among the side chains.

The d spacing changes in 17iPC are certainly associated with hydration of the head group region, and probably by a concomitant conformation change. We also observe a coexistence of the two gel phases over a several degree interval.

In 20iPC, an increase in d spacing is expected as the chains orient along the bilayer normal during the transition. The effective length of a CH_2 group is 1.25 Å so the length of a 20iPC side chain in the all-*trans* conformation is ~24 Å. Rotation from a 33° cant to normal orientation leads to a bilayer increase of $2 \times 4 = 8$ Å. The observed increase (5.4 Å) is definitely less than expected from these side chain factors, implying that the subgel to gel phase transition in 20iPC is accompanied by changes in the interfacial region.

In qualitative terms, it seems clear that the 17iPC hydrates somewhat while the 20iPC dehydrates somewhat so both their head group and acyl chain states become more similar in their gel phases. This is consistent with IR data, which show spectral features of loosely packed chain structures in which the chains are rotationally disordered and moving independently of each other. The IR bands become more similar (the 1,716 cm^{-1} band in 20iPC disappears) and the ^{31}P NMR shows similar head group

mobility (increased over the rigid lattice patterns of the subgel phases) (3).

It has been shown that the subgel phases of 17iPC and 20iPC differ in side chain cant angle, but that their side chain states in the gel phase are more similar. However, there are also important differences between the two gel phases that are not reflected by the wide angle data. The signal to noise ratio in lamellar reflections in 17iPC is significantly greater than that in 20iPC. This difference is due to a diffuse x-ray scattering in the 20iPC homolog. It is difficult to make quantitative deductions from this diffuse scattering, but its presence indicates a lesser degree of lamellar order in the gel phase of the longer chain homolog.

Liquid Crystal Phases

Upon further heating, both 17iPC and 20iPC undergo a final phase transition in which the *d* spacings increase and sharp reflections in the wide angle region are lost. The wide angle region is now characterized by a broad reflection (very weakly visible) at 1/4.4 to 1/4.5 $Å^{-1}$. This is the signature of a liquid crystal Lα phase.

It is noteworthy that the *d* spacing of 17iPC increases dramatically by 6.0 Å at T_{gl}. This large change clearly signals a pronounced increase in hydration state of this homolog. The side chains melt and their effective bilayer length decreases, so the water region must increase by at least 10 Å. By contrast, in 20iPC the increase in *d* spacing is only ~5 Å. In this case, it is possible that the greater decrease in hydrocarbon thickness, occurring because a longer chain melts, more nearly counteracts the increase in water layer thickness.

CONCLUSIONS

The analysis presented above provides a clear picture of the lamellar and intralamellar structures in 17iPC and 20iPC, some features of which are shown schematically in Fig. 8. In the subgel phase the two homologs differ in long and short range order, as well as in both the hydrophobic and the interfacial regions. However, the two-dimensional molecular lattices within the bilayer planes are related. Indeed, the side chain canting of 20iPC occurs within a plane containing a unit cell vector identified in both 17iPC and 20iPC. The gel phases in both species are similar in their side chain arrangements, but the 20iPC has a more disordered lamellar structure and there are differences in the headgroup-water interface region. At the gel to liquid crystal phase transition, both lipid dispersions exhibit side chain melting. The very large changes in *d* spacing at T_{gl} reflect side chain melting and major changes in the interfacial head group region. These changes are greater in iPCs than in nPCs, illustrating the rather dramatic effects that modest variation in lipid molecular structure can have on their thermotropic behavior (22).

It is a pleasure to thank Ted LaPage for assistance with computer programs used in this work.

This research was supported in part by National Insitute of Environmental Health Services grant ES00040, and National Institutes of Health Biomedical Research Support grant RR07079.

Received for publication 14 September 1985 and in revised form 14 October 1985.

REFERENCES

1. Silvius, J. R., and R. N. McElhaney. 1979. Effects of phospholipid acyl chain structure on physical properties 1. Isobranched phosphatidylcholines. *Chem. Phys. Lipids.* 24:287–296.
2. Lewis, R. N. A. H., and R. N. McElhaney. 1985. The thermotropic phase behavior of model membranes composed of phosphatidylcholines containing methyl isobranched fatty acids. I. Differential scanning calorimetry studies. *Biochemistry.* 24:2431–2439.
3. Mantsch, H. H., C. Madec, R. N. A. H. Lewis, and R. N. McElhaney. 1985. The thermotropic behavior of model membranes composed of phosphatidylcholines containing isobranched fatty acids II. Infrared and ^{31}P-NMR studies. *Biochemistry.* 24:2440–2446.
4. Kannenberg, E., A. Blume, R. N. McElhaney, and K. Poralla. 1983. Monolayer and calorimetric studies of phosphatidylcholines containing branched-chain fatty acids and of their interactions with cholesterol and with a bacterial hopanoid in model membranes. *Biochem. Biophys. Acta.* 733:111–116.
5. Kaneda, T. 1977. Fatty acids of the genus bacillus: an example of branched chain preference. *Bacteriol. Revs.* 75:711–733.
6. Tardieu, A., V. Luzzati, and F. C. Reman. 1973. Structure and polymorphism of the hydrocarbon chains of lipids: a study of lecithin-water phases. *J. Mol. Biol.* 15:4575–4580.
7. Janiak, M. J., D. M. Small, and B. J. Shipley. 1980. Nature of the thermal pretransition of synthetic phospholipids: dimyristoyl- and dipalmitoyllecithin. *Biochemistry.* 15:4575–4580.
8. Chen, S. C., J. M. Sturtevant, and B. J. Gaffney. 1980. Scanning calorimetric evidence for a third phase transition in phosphatidylcholine bilayers. *Proc. Natl. Acad. Sci. USA.* 77:5060–5063.
9. Füldner, H. H. 1981. Characterization of a third phase transition in multilamellar dipalmitoyllecithin liposomes. *Biochemistry.* 20:5707–5710.
10. Ruocco, M. J., and G. G. Shipley. 1982. Characterization of the sub-transition of hydrated dipalmitoylphosphatidylcholine bilayers. X-ray diffraction study. *Biochim. Biophys. Acta.* 684:59–66.
11. Ruocco, M. J., and G. G. Shipley. 1982. Characterization of the sub-transition of hydrated dipalmitoylphosphatidylcholine bilayers. Kinetic, hydration and structural study. *Biochim. Biophys. Acta.* 691:309–320.
12. Stümpel, J., H. Eibl, and A. Nicksch. 1983. X-ray analysis and calorimetry on phosphatidylcholine model membranes. *Biochim. Biophys. Acta.* 727:246–254.
13. Nagle, J. F., and D. A. Wilkinson. 1982. Dilatometric studies of the subtransition in dipalmitoylphosphatidylcholine. *Biochemistry.* 21:3817–3821.
14. Luzzati, V. 1968. X-ray diffraction studies of lipid-water systems. *Biological Membranes.* 1:71–123.
15. Ranck, J. L. 1983. X-ray diffraction studies of the phase transitions of hydrocarbon chains in bilayer systems: statics and dynamics. *Chem. Phys. Lipids.* 32:251–270.
16. Lytz, R. K. 1978. X-ray structure studies of oriented phospholipid multilayers. Ph.D. thesis. Oregon State University, Corvallis, OR.
17. Hui, S. W. 1976. The tilting of the hydrocarbon chains in a single bilayer of phospholipid. *Chem. Phys. Lipids.* 16:9–18.
18. Sakurai, I., T. Sakurai, T. Seto, and S. Iwayanagi. 1983. Lyotropic

phase transitions in single crystals of L- and DL-dipalmitoylglycerophosphocholines. *Chem. Phys. Lipids.* 32:1–11.

19. Mushayakarara, K., and I. W. Levin. 1982. Determination of acyl chain conformation at the lipid interface region: Raman spectroscopic study of the carbonyl stretching mode region of dipalmitoylphosphatidylcholine and structurally related molecules. *J. Phys. Chem.* 86:2324–2327.
20. Cameron, D. G., and H. H. Mantsch. 1982. Metastability and polymorphism in the gel phase of 1,2-dipalmitoyl-3-*sn*-phosphatidylcholine. *Biophys. J.* 38:175–184.
21. Abrahamsson, S. 1959. On the crystal structure of 17-methyloctadecanoic acid. *Arkiv foer Kemi.* 14:49–55.
22. Lytz, R. K., J. C. Reinert, S. E. Church, and H. H. Wickman. 1984. Structural properties of a monobrominated analog of 1,2-dipalmitoyl-*sn*-glycero-3-phosphorylcholine. *Chem. Phys. Lipids.* 35:63–76.